Geochimica et Cosmochimica Acta, Vol. 68, No. 24, pp. 5197–5204, 2004

0016-7037/04 $30.00 + .00

doi:10.1016/j.gca.2004.06.006

Measuring quartz solubility by in situ weight-loss determination using a hydrothermal diamond cell

HALAN M. WANG,* GRANT S. HENDERSON, and JAMES M. BRENAN
University of Toronto, Department of Geology, 22 Russell Street, Toronto, ON, M5S 3B1, Canada

(*Received January* 15, 2004; *accepted in revised form June* 15, 2004)

Abstract—The solubility of quartz was determined using a hydrothermal diamond anvil cell (HDAC) within the temperature and pressure ranges of 126 to 490°C and up to 8.9 kbar, respectively. A novel approach has been used to measure the amount of dissolved silica. The quartz was abraded into spheres which have a diameter of ~40 μm. The spheres were then placed in pure water inside the diamond anvil cell and heated externally. Because the transparency of the diamonds allows direct observation of the sample chamber during the experiment, we were able to estimate the amount of quartz dissolved in the water at various stages of the dissolution process by measuring the decrease in the sphere's diameter over time. Experiments were performed along isochores between 0.92 and 0.99 g/cm^3. The maximum solubility measured was 0.165 molal. The experimental solubility data were limited to 370°C because of overestimation of solubilities above this temperature. Reprecipitation of silica inside the HDAC sample chamber and the refaceting of the spheres to trigonal form at temperatures above 350°C are major contributors to the overestimation. *Copyright © 2004 Elsevier Ltd*

1. INTRODUCTION

Numerous studies have reported the solubility of quartz in aqueous systems. The first comprehensive study was made by Kennedy (1950) whose experiments spanned a temperature range of 160 to 610°C and a pressure range of 6.2 to 1750 bars. Subsequent investigations have expanded the solubility region to include very low temperature measurements from 25° to 300°C at ambient pressure to liquid-vapor saturation (Van Lier et al., 1960; Morey et al., 1962; Siever, 1962; Rimstidt, 1997) and, very high temperature and pressure measurements up to 900°C and 20 kbar (Anderson and Burnham, 1965; Manning, 1994).

Solubility experiments have always been performed in closed vessels. Hydrothermal pressure autoclaves, for example, have been used extensively to determine silica solubility (Kennedy, 1950; Morey and Hesselgesser, 1951a,b; Brady, 1953; Frederickson and Cox, 1954; Smith, 1958; Kitahara, 1960a,b; Laudise and Ballman, 1961; Kennedy et al., 1962; Morey et al., 1962; Siever, 1962; Weill and Fyfe, 1964; Anderson and Burnham, 1965; Sommerfeld, 1967; Semenova and Tsiklis, 1970; Rimstidt, 1997). The amount of quartz dissolved into solution is determined either by weighing the sample before and after the experimental run, or analyzing the solution for dissolved silica by chemical titration or by spectrophotometric methods.

However, these methods possess several disadvantages. For example, temperature gradients within the reaction vessel itself affect mineral dissolution by initiating dissolution at the hotter end of the autoclave, and precipitation at the cooler end (Mizutani, 1966). Furthermore, the quench process carries with it the possibility of reaction between the undissolved solid phase and the solution as the system is cooled (Walther and Orville, 1983). The loss of sample due to precipitation during cooling cannot be measured accurately, nor is it possible to confirm whether any of the reprecipitated sample is a quench product (Friedman, 1948; Von Damm et al., 1991). This is despite improvements in quench techniques that reduce quench times from a scale of minutes to seconds (Manning, 1994).

Extraction devices have also been used to remove small aliquots of solution from the reaction vessel at experimental conditions (Morey and Hesselgesser, 1951; Walther and Orville, 1983). This technique avoids any back-reaction between the solution and sample and allows the solution to be analyzed immediately. However, precipitation of silica may still occur because of the sudden changes in temperature and pressure during extraction (Fournier and Potter, 1982).

The hydrothermal diamond anvil cell (HDAC) possesses a unique design which allows in situ measurements of the sample during an experiment (Bassett et al., 1993). The HDAC is a small, compact instrument holding two diamonds (Fig. 1). The transparency of the diamonds to light allows direct observation of the sample and the aqueous medium which are held inside a rhenium gasket between the two diamond faces. The sample chamber can easily be viewed under a microscope and analyzed by optical techniques. A study by Zotov and Keppler (2002) presented silica solubility results determined by Raman spectroscopy in an HDAC up to 900°C and 14 kbar. By correlating the intensity of the silica bands to the molality of dissolved silica, they were able to reproduce molalities published by both Fournier and Potter (1982) and Manning (1994) up to 11 kbar. However, this method is only applicable so long as the silica bands are detectable. Zotov and Keppler (2002) show a lower limit of 400°C for a bulk density, $\rho = 0.82$ g/cm^3 and 300°C for $\rho = 0.92$ g/cm^3. Moreover, the signal-to-noise ratio is reduced at lower temperatures and pressures making it difficult to obtain accurate integration. An alternative method is therefore needed to measure quartz solubility below these temperatures. This study presents quartz solubility data collected in an HDAC

* Author to whom correspondence should be addressed (halan@geology.utoronto.ca).

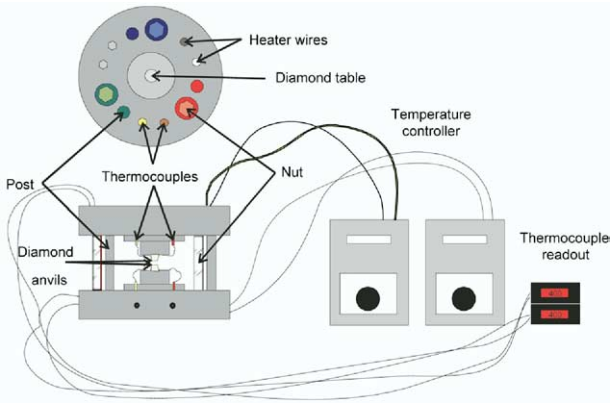

Fig. 1. Schematic of the hydrothermal diamond anvil cell (HDAC). Features are not to scale.

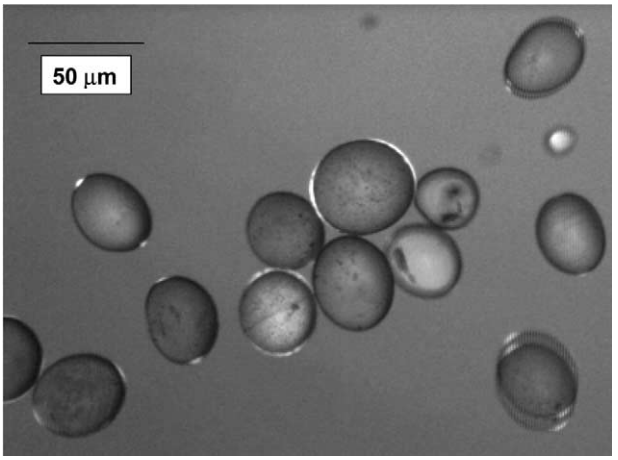

Fig. 2. Quartz spheres with average diameter of 40 μm used in our solubility experiments.

between 25° and 490°C and 1 bar to 8.9 kbar by measuring the diameter of the dissolving quartz sample from digital images to estimate the loss of quartz mass in solution. And although the advent of the HDAC has made in situ measurements possible, the results presented below also expose several disadvantages of the method which must be improved upon if it is to be used as a reliable tool for solubility experiments.

2. EXPERIMENTAL METHOD

The solubility experiments were carried out in a Bassett-type hydrothermal diamond anvil cell (Bassett et al., 1993). The sample and fluid are held together in a rhenium gasket between the two nonfluorescing diamond faces (Fig. 1). The dimensions of the sample chamber are controlled by the thickness of the rhenium gaskets (125 μm) and the diameter of the gasket hole (500 μm). The diamonds are supported by tungsten carbide seats which also house the heating components of the cell. Chromel wire wraps around the seats and externally heats the diamonds by applying an electrical current. Separate temperature controllers are used for the upper and lower diamonds. The temperature inside the sample chamber is gauged by two separate thermocouples which are cemented to the side of each diamond. Temperature calibration is achieved by determining the melting points of $NaNO_3$ (T_m = 306.8°C) and NaCl (T_m = 800.5°C) inside the HDAC. The temperature difference between the upper and lower diamonds did not exceed more than an average of ±2°C with a maximum temperature difference of ±5°C although this value increased to ±10°C at temperatures above 400°C, depending on the condition of the chromel heating wires. A stainless steel cylindrical sheath encloses the contents of the HDAC into which a gas mixture of 1% H_2 in Ar is introduced to prevent the oxidation of the heating components and the diamonds.

Natural quartz samples were used in the solubility experiments. First, rounded grains of quartz with an initial diameter of ~100 μm, were plucked from a previously crushed quartzite sample obtained from northern Ontario, and then abraded under an air current of 3.5 psi for roughly 100 h. Pyrite was used as the polishing agent. Abrasion yielded very smooth and well-rounded quartz ellipsoids (which we have called "spheres") with a mean diameter of ~40 μm (Fig. 2). The quartz "spheres" were washed in boiling HNO_3 to remove any excess pyrite on the surface, and cleaned with ethanol before loading into the HDAC. Both synthetic quartz and Brazilian quartz were also considered for abrasion but these samples yielded very angular and prismatic grains when initially crushed and produced football- or disk-shaped ellipsoids after prolonged abrasion. This type of morphology was not suitable for our method of mass estimation and these grains were discarded.

In each solubility experiment, the HDAC was loaded with a single quartz sphere, distilled and deionized water and a vapor bubble. The rhenium gasket was conditioned by heating and cooling the sample chamber several times until the vapor bubble disappeared at a constant temperature of homogenization. This temperature determined the bulk density of the water in the chamber. Pressure was then estimated along the respective isochore as governed by the equation of state of water (Saul and Wagner, 1989). The error in the homogenization temperature is estimated to be ±5°C. Movement of the quartz sphere was not observed within the sample chamber except during the temperature homogenization process. Occasionally, the vapor bubbles would push the sample to the side of the gasket in which case the experiment was usually terminated if the view of the sphere diameter was skewed. Otherwise, the sample typically sat on the bottom diamond surface and remained stationary throughout the experiment. The diamond surfaces were thoroughly cleaned with ethanol between experiments and aligned as needed.

Direct weighing of the quartz grains using a microbalance was found to be extremely difficult and tedious. Moreover, the grains weighed less than the precision of the balance (±1 μg). Therefore, the mass of each quartz sphere was calculated based on the lengths of the two principal axes. This method of "optical weighing" was adopted from a method used for determining the mass of very small zircon grains (~ 100 μm) (Matthews and Davis, 1999). In the case of zircons, the accuracy of this method was ±10% of the weighed value for grains with an aspect ratio between 1:1 and 3:1. Prismatic and pointed zircon grains were not suitable candidates for this method because of overestimation of the true mass, whereas the more rounded and ellipsoidal grains yielded calculated weights within the calibrated range. Therefore, we abraded quartz spheres to an ellipsoidal morphology with a typical aspect ratio of 1:1.

For each experiment, multiple measurements were made of the quartz sphere in several different orientations before the start of each experiment at room temperature to ensure an accurate initial mass. The HDAC was then loaded with the quartz sphere and water, and the gasket was conditioned to a suitable bulk density. The sample chamber was then slowly heated to a given temperature and the sample left to equilibrate for up to 15 min. The temperature of the HDAC was then slowly raised again and left to equilibrate. This procedure was continued until the quartz sphere was completely dissolved into solution. Throughout the heating of the HDAC, digital images of the quartz sphere were taken using a 10× long working distance objective at each temperature interval. The optic path was oriented vertically from the top diamond surface to the bottom diamond surface. The loss of mass was estimated by measuring the decrease in the length of the two elliptical axes.

The volume of water in the HDAC could not be measured directly. Instead, we assumed that the amount of water was equal to the dimensions of the sample chamber. Compression of the rhenium gasket was also considered in the calculations although the change in thickness of the gasket was presumed to decrease the total sample chamber volume by 0.5% (Bassett et al., 1993). The corrected water volume represented only a difference of 0.5% of the original calculated volume.

Table 1. Experimental results.

Temperature (°C)	P (kbar)	Volume of water (mL)	Quartz loss (μg)	Solubility (ppm)
Bulk density ρ = 0.92; homogenization temperature T_h = 150° ± 5°C				
227	1.4	0.02222 ± 0.00002	0.0119 ± 0.0023	535 ± 115
252	1.9		0.0158 ± 0.0022	709 ± 122
276	2.3		0.0185 ± 0.0022	834 ± 129
290	2.6		0.0211 ± 0.0021	950 ± 135
313	3.0		0.0266 ± 0.0021	1199 ± 152
331	3.3		0.0315 ± 0.0020	1417 ± 168
354	3.8		0.0476 ± 0.0018	2141 ± 228
370	4.1		0.0665 ± 0.0014	2992 ± 306
394	4.5		0.0872 ± 0.0011	3927 ± 396
395	4.5		0.0932 ± 0.0009	4197 ± 422
227	1.4	0.02378 ± 0.00002	0.0073 ± 0.0041	307 ± 175
263	2.1		0.0143 ± 0.0040	600 ± 180
285	2.5		0.0217 ± 0.0039	913 ± 189
287	2.5		0.0218 ± 0.0039	916 ± 190
311	3.0		0.0236 ± 0.0039	993 ± 192
329	3.3		0.0301 ± 0.0039	1266 ± 206
350	3.7		0.0465 ± 0.0037	1955 ± 249
378	4.2		0.0708 ± 0.0034	2978 ± 330
Bulk density p = 0.94; homogenization temperature = 125° ± 5°C				
203	1.4	0.02223 ± 0.00002	0.0088 ± 0.0026	395 ± 122
228	1.9		0.0093 ± 0.0026	417 ± 123
264	2.6		0.0188 ± 0.0024	844 ± 138
279	2.9		0.0182 ± 0.0024	820 ± 137
333	3.9		0.0388 ± 0.0021	1745 ± 198
354	4.3		0.0456 ± 0.0020	2050 ± 223
371	4.7		0.0602 ± 0.0018	2706 ± 282
391	5.0		0.0670 ± 0.0017	3015 ± 311
392	5.0		0.0883 ± 0.0013	3970 ± 401
394	5.1		0.0822 ± 0.0015	3699 ± 376
395	5.1		0.0974 ± 0.0012	4381 ± 441
Bulk density p = 0.97; homogenization temperature = 80° ± 5°C				
132	0.8	0.02195 ± 0.00002	0.0062 ± 0.0032	284 ± 148
171	1.5		0.0052 ± 0.0032	250 ± 147
204	2.2		0.0116 ± 0.0031	528 ± 152
238	2.9		0.0108 ± 0.0031	494 ± 151
274	3.6		0.0146 ± 0.0031	667 ± 156
310	4.4		0.0273 ± 0.0027	1245 ± 180
332	4.8		0.0357 ± 0.0027	1628 ± 205
357	5.3		0.0523 ± 0.0025	2384 ± 265
358	5.3		0.0564 ± 0.0025	2569 ± 280
381	5.8		0.0836 ± 0.0021	3810 ± 393
392	6.0		0.1087 ± 0.0017	4950 ± 501
415	6.5		0.1229 ± 0.0015	5598 ± 564
183	1.7	0.02329 ± 0.00002	0.0051 ± 0.0035	220 ± 153
216	2.4		0.0082 ± 0.0035	353 ± 154
248	3.1		0.0148 ± 0.0034	634 ± 160
274	3.6		0.0318 ± 0.0032	1364 ± 194
304	4.2		0.0240 ± 0.0039	1029 ± 196
335	4.9		0.0396 ± 0.0037	1701 ± 233
348	5.1		0.0540 ± 0.0036	2318 ± 278
367	5.5		0.0827 ± 0.0032	3552 ± 381
403	6.3		0.1175 ± 0.0028	5044 ± 519
417	6.6		0.1461 ± 0.0025	6274 ± 636
197	2.0	0.02300 ± 0.00002	0.0043 ± 0.0032	188 ± 140
225	2.6		0.0097 ± 0.0031	422 ± 142
250	3.1		0.0164 ± 0.0030	711 ± 147
278	3.7		0.0194 ± 0.0029	845 ± 153
293	4.0		0.0239 ± 0.0029	1041 ± 163
336	4.9		0.0368 ± 0.0027	1599 ± 199
354	5.3		0.0515 ± 0.0025	2240 ± 250
374	5.7		0.0684 ± 0.0023	2972 ± 314
387	5.9		0.0785 ± 0.0022	3411 ± 354
410	6.4		0.1118 ± 0.0017	4860 ± 492
419	6.6		0.1285 ± 0.0014	5585 ± 562
427	6.8		0.1411 ± 0.0012	6136 ± 616
200	2.1	0.02098 ± 0.00002	0.0027 ± 0.0041	128 ± 194

Table 1. Continued.

Temperature (°C)	P (kbar)	Volume of water (mL)	Quartz loss (· g)	Solubility (ppm)
219	2.5		0.0235 ± 0.0039	1120 ± 215
256	3.2		0.0252 ± 0.0038	1202 ± 219
285	3.8		0.0366 ± 0.0037	1746 ± 249
305	4.2		0.0295 ± 0.0038	1407 ± 229
326	4.7		0.0376 ± 0.0037	1790 ± 252
365	5.5		0.0452 ± 0.0036	2154 ± 276
395	6.1		0.0803 ± 0.0032	3825 ± 413
413	6.5		0.0891 ± 0.0031	4247 ± 450
431	6.9		0.1275 ± 0.0027	6076 ± 621
444	7.1		0.1569 ± 0.0023	7479 ± 756
448	7.2		0.1744 ± 0.0020	8310 ± 837
Bulk density $\rho = 0.99$; homogenization temperature = 50° ± 5°C				
202	2.7	0.02450 ± 0.00002	0.0122 ± 0.0023	500 ± 107
255	3.8		0.0136 ± 0.0023	556 ± 109
322	5.3		0.0504 ± 0.0018	2055 ± 218
150	1.7	0.02359 ± 0.00002	0.0035 ± 0.0041	148 ± 173
295	4.7		0.0291 ± 0.0040	1234 ± 208
321	5.3		0.0373 ± 0.0039	1580 ± 228
355	6.0		0.0580 ± 0.0036	2459 ± 290
384	6.6		0.0834 ± 0.0033	3535 ± 381
406	7.1		0.1174 ± 0.0029	4975 ± 513
435	7.7		0.1805 ± 0.0021	7651 ± 770
453	8.1		0.2340 ± 0.0011	9919 ± 993
162	1.9	0.02428 ± 0.00002	0.0032 ± 0.0038	132 ± 156
205	2.8		0.0054 ± 0.0037	221 ± 155
251	3.8		0.0106 ± 0.0037	435 ± 158
301	4.8		0.0301 ± 0.0035	1240 ± 189
345	5.8		0.0548 ± 0.0035	2256 ± 267
381	6.6		0.0779 ± 0.0032	3209 ± 347
395	6.9		0.1014 ± 0.0029	4175 ± 434
410	7.2		0.1045 ± 0.0028	4303 ± 446
425	7.5		0.1015 ± 0.0028	4179 ± 434
451	8.1		0.1034 ± 0.0028	4259 ± 442
462	8.3		0.1034 ± 0.0028	4259 ± 442
490	8.9		0.1139 ± 0.0027	4690 ± 482
126	1.2	0.02158 ± 0.00002	0.0065 ± 0.0037	302 ± 174
199	2.6		0.0098 ± 0.0037	456 ± 176
235	3.4		0.0149 ± 0.0036	688 ± 181
261	4.0		0.0196 ± 0.0043	907 ± 219
298	4.8		0.0302 ± 0.0042	1397 ± 240
315	5.1		0.0430 ± 0.0041	1995 ± 275
338	5.6		0.0507 ± 0.0040	2350 ± 299
384	6.6		0.0920 ± 0.0036	4265 ± 457
402	7.0		0.1209 ± 0.0033	5601 ± 580
128	1.2	0.02298 ± 0.00002	0.0031 ± 0.0028	133 ± 120
170	2.0		0.0041 ± 0.0027	179 ± 120
219	3.1		0.0102 ± 0.0027	442 ± 124
253	3.8		0.0133 ± 0.0026	580 ± 128
282	4.4		0.0229 ± 0.0024	997 ± 146
334	5.5		0.0337 ± 0.0023	1466 ± 178
361	6.1		0.0650 ± 0.0019	2828 ± 294
387	6.7		0.0814 ± 0.0016	3542 ± 361
399	7.0		0.0968 ± 0.0014	4211 ± 425
416	7.3		0.1119 ± 0.0011	4870 ± 489
191	2.5	0.02283 ± 0.00002	0.0042 ± 0.0041	186 ± 181
227	3.2		0.0072 ± 0.0041	316 ± 182
257	3.9		0.0159 ± 0.0040	697 ± 188
288	4.5		0.0318 ± 0.0037	1395 ± 215
321	5.3		0.0294 ± 0.0038	1287 ± 209
331	5.5		0.0486 ± 0.0036	2131 ± 265
373	6.4		0.0866 ± 0.0032	3793 ± 404
388	6.7		0.1161 ± 0.0028	5084 ± 523
402	7.0		0.1547 ± 0.0024	6777 ± 686
414	7.3		0.1667 ± 0.0022	7303 ± 737
427	7.6		0.1861 ± 0.0020	8154 ± 820

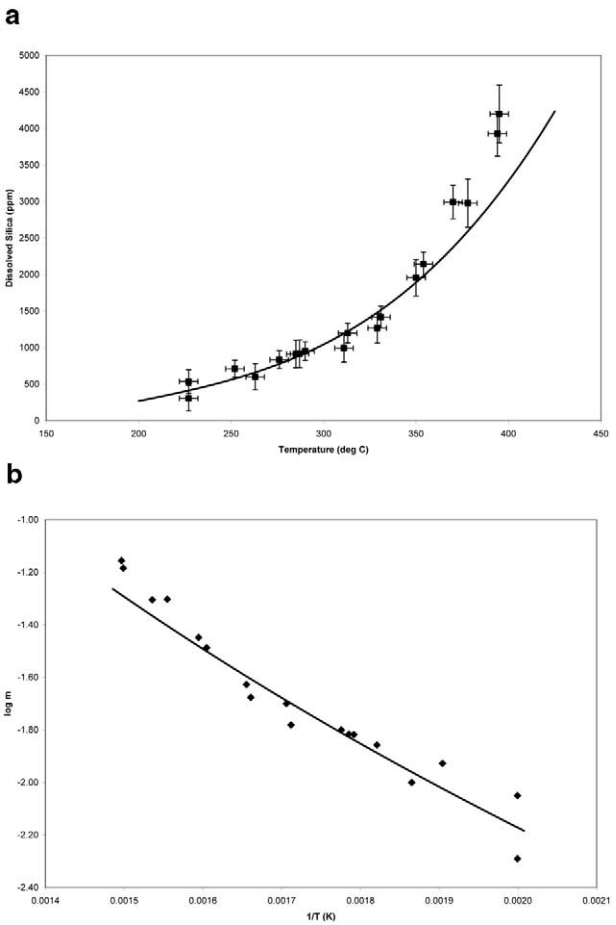

Fig. 3. (a) Solubility curve for isochoric experiments at $\rho = 0.92$ g/cm^3. Squares represent experimental data; solid line represents calculated solubility (Manning, 1994). The horizontal error bars represent the error in temperature. The vertical error bars represent the error in solubility. (b) Solubility data plotted as log m vs. 1/T. Diamonds represent experimental data; solid line represents calculated solubility.

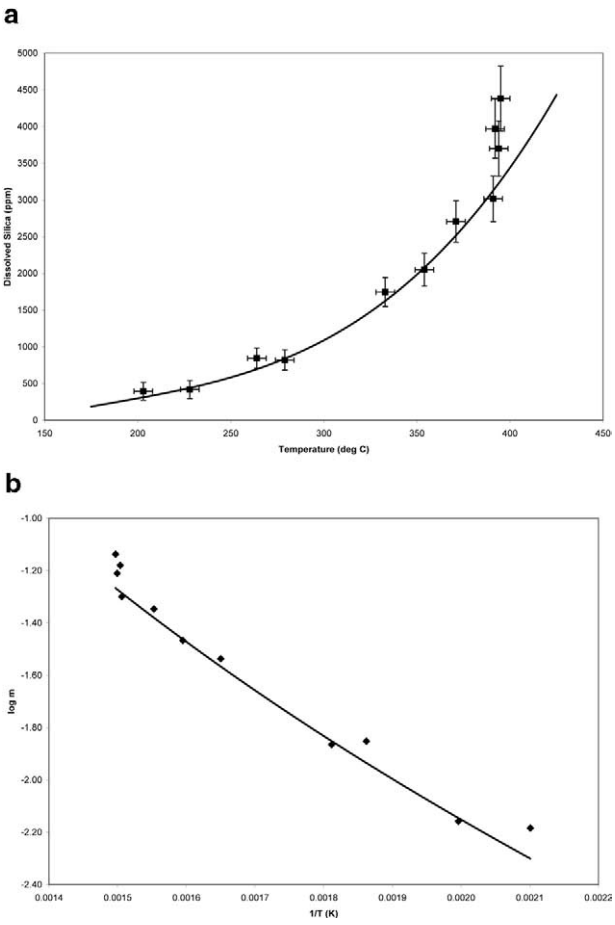

Fig. 4. (a) Solubility curve for isochoric experiments at $\rho = 0.94$ g/cm^3. Squares represent experimental data; solid line represents calculated solubility (Manning, 1994). The horizontal error bars represent the error in temperature. The vertical error bars represent the error in solubility. (b) Solubility data plotted as log m vs. 1/T. Diamonds represent experimental data; solid line represents calculated solubility.

3. RESULTS AND DISCUSSION

Solubility data were collected between a temperature range of 126° to 490°C and a pressure range up to 8.9 kbar for bulk densities of 0.92, 0.94, 0.97 and 0.99 g/cm^3. The results are summarized in Table 1 and plotted in Figures 3 through 6. The squares show the results of this study and are compared to solubility curves calculated using the data of Manning (1994). His equilibrium constant expression for the solubility of quartz encompasses the largest range of temperature (25° to 900°C) and pressure (to 20 kbar) and includes several studies performed at experimental conditions similar to ours. Our temperature measurements have a maximum error of ±5°C which increases to ±10°C for measurements above 400°C. The error in the quartz mass is smaller than ±0.0043 μg and translates into an error in the quartz solubility of ~10% or less at any given temperature. This error is based on the accuracy of the quartz diameter measurements taken from the digital images. We have assumed a measuring error of one pixel (or 0.535 μm) for each principal axis. The precision of the experimental solubilities was not calculated because of the lack of replicate measurements at specific temperatures and pressures.

Our quartz solubility data appear to agree well with published data (Manning, 1994). For any given isochoric experiment, the solubility increases with increasing temperature, as predicted by previous studies (Kennedy, 1950; Manning, 1994). However, with the exception of the 0.94 g/cm^3 isochore, the data begin to deviate at ~370°C. Below 370°C, the results exhibit fairly narrow scattering above and below the expected solubility curves. Discrepancies may be attributed to errors in the estimations of the quartz mass by the optical weighing program from 2D measurements. The quality of the digital images has a great influence on the accuracy of the quartz mass. For example, a poorly focused sphere or the appearance of shadows in the images can increase the error in the diameter measurement by more than one percent. In a few cases, anomalously high solubilities are observed despite any apparent flaws in the images (Fig. 5).

Waiting times of several minutes to a quarter of an hour were also used to allow the diamond heaters to correct any temperature imbalances, and to allow the solution to reach equilibrium concentrations. Zotov and Keppler (2002) have shown through time-dependent measurements in the HDAC that the equilib-

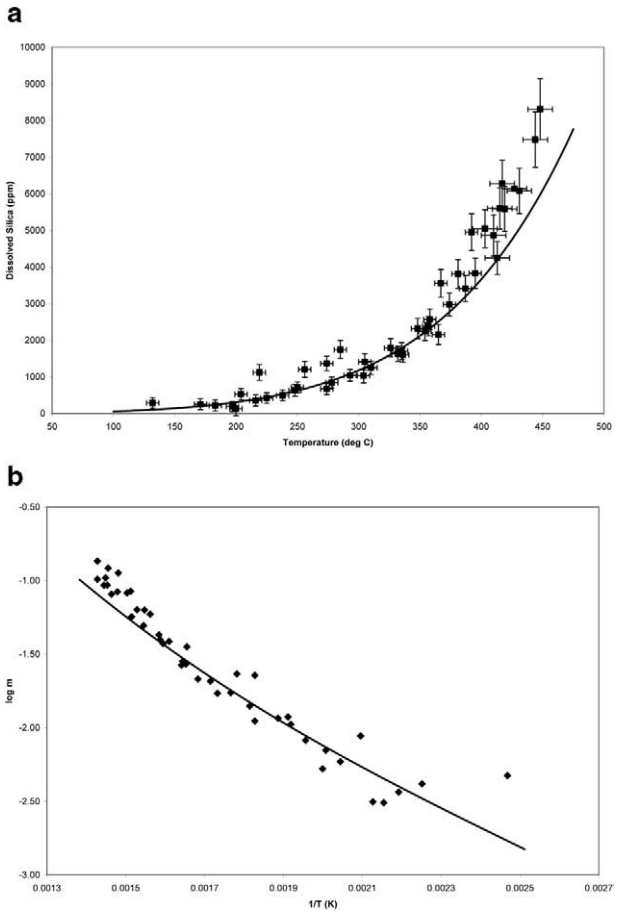

Fig. 5. (a) Solubility curve for isochoric experiments at $\rho = 0.97$ g/cm^3. Squares represent experimental data; solid line represents calculated solubility (Manning, 1994). The horizontal error bars represent the error in temperature. The vertical error bars represent the error in solubility. (b) Solubility data plotted as log m vs. 1/T. Diamonds represent experimental data; solid line represents calculated solubility.

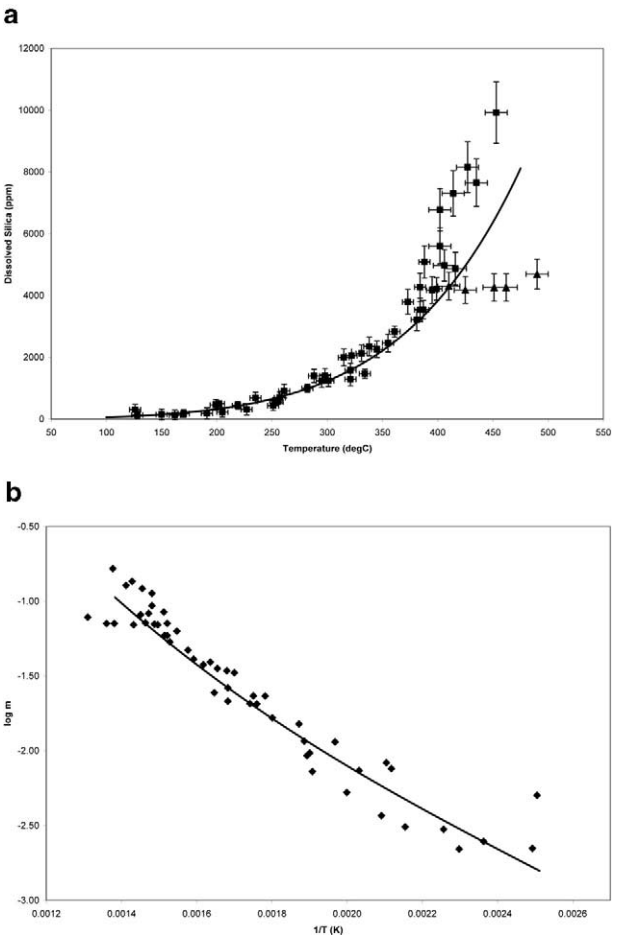

Fig. 6. (a) Solubility curve for isochoric experiments at $\rho = 0.99$ g/cm^3. Squares and triangles represent experimental data; solid line represents calculated solubility (Manning, 1994). The horizontal error bars represent the error in temperature. The vertical error bars represent the error in solubility. (b) Solubility data plotted as log m vs. 1/T. Diamonds represent experimental data; solid line represents calculated solubility.

rium concentration of the dissolved quartz is achieved seconds after heating to the respective temperature. Although this observation applies to temperatures above 400°C, it is also important to note that they include experimental data as low as 200°C, and accumulation times as short as several minutes for temperatures below 800°C. Moreover, while kinetic studies by Rimstidt and Barnes (1980) appear to require longer waiting times at lower temperatures, our results do not exhibit grossly underestimated solubilities in the lower temperature region, and in fact display scattering above the established solubility curve, suggesting that our waiting times were sufficiently long for equilibrium to occur.

The detection limit varied with each isochoric experiment. The measurable solubilities were obtained at progressively lower temperature with increasing bulk density (pressure) since quartz solubility is strongly pressure dependent. The lowest temperature recorded was at 126°C for the 0.99 g/cm^3 bulk density experiments, and increased to 227°C for the 0.92 g/cm^3 bulk density experiments. Solubility measurements were also limited by the initial diameter of the quartz sphere. In general, the smaller the initial diameter of the sphere, the larger the initial changes in diameter were needed to be observed under the microscope. The use of a higher-powered objective lens may improve the measurements especially at very low temperatures (<200°C) and lower bulk densities ($\rho < 0.97$ g/cm^3). The precision or reproducibility of our measurements at specific temperature and pressure intervals was not tested in any of our experiments. However, we did vary the diameters and mass of our quartz spheres for each of the isochores, with the exception of $\rho = 0.94$ g/cm^3 for which only one experiment was included. For $\rho = 0.92$ g/cm^3, the initial masses ranged between 0.1221 and 0.2700 μg; for $\rho = 0.97$ g/cm^3, the initial masses ranged between 0.1822 and 0.2678 μg and for $\rho = 0.99$ g/cm^3, the initial masses ranged between 0.1251 and 0.2707 μg. Despite the variation in grain size, we were able to obtain similar solubility results at each bulk density.

At temperatures above 370°C, the solubility values consistently plot well above the established solubility curve, suggesting that more quartz is dissolving into solution than expected. However, upon closer inspection of the digital images, very tiny grains of quartz, as identified by Raman spectroscopy,

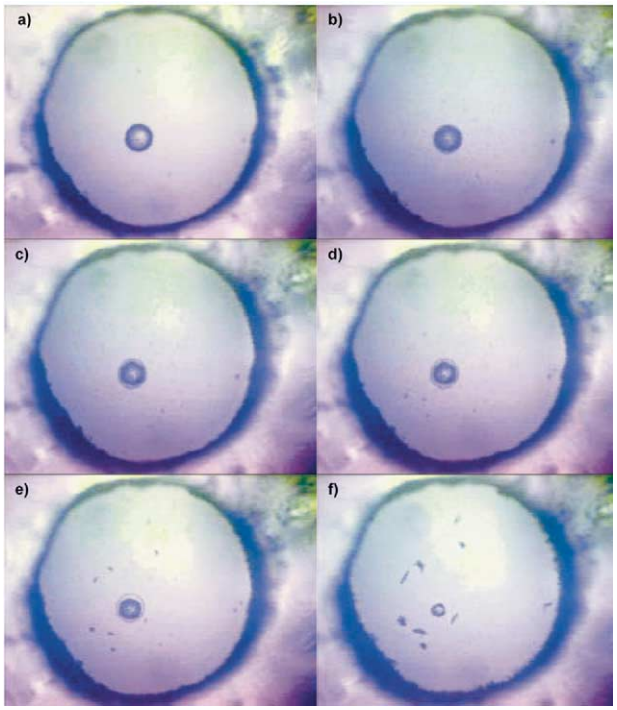

Fig. 7. Panels a through f show a progression of a solubility experiment performed at $\rho = 0.99$ g/cm^3. (a) 150°C. (b) 295°C. (c) 355°C. (d) 384°C. (e) 406°C. (f) 453°C. No reprecipitation of silica is noted in (a) and (b). Tiny grains begin to appear in (c) and continue to grow larger through (d) to (f). Faceting of the dissolving quartz sphere is observed in (c).

were precipitating onto the diamond faces above this temperature (Fig. 7). This reprecipitation is most likely due to a thermal gradient present within the sample chamber. However, dissolution of the reprecipitated quartz grains could not be achieved even with the "overheating" of either the upper or lower diamond surface to compensate for the thermal gradient. Unfortunately, the major drawback of the optical weighing method is that there is no accurate way of determining the amount of reprecipitation in the cell at the present time. The crystals are often too small and too many in number to estimate the recovered mass. It is also difficult to determine how many of the microcrystals have planted themselves on the gasket wall, let alone the diamond faces. Furthermore, the optical weighing technique is designed for spherical objects and is not suitable for long, prismatic crystals (Matthews and Davis, 1999), the habit observed for the newly grown silica phase.

There is little information on the morphology of quartz grains during dissolution (Heimann et al., 1970; Manning, 1994). Heimann et al. (1970) found that the quartz spheres formed highly curved faces and edges. Flat faces and flat edges were not attained until 95% of the initial quartz mass had dissolved into solution. Because digital images were taken throughout each experiment, we were able to observe the dissolution effects on the surface of the quartz spheres as well. Typically, the quartz sphere refacets its crystal faces (becomes trigonal) during heating, the onset of which occurs at approximately ~350 to 360°C. Figure 7 shows the progression of the faceting as the quartz sphere assumes the trigonal form inside the HDAC. This phenomenon, coupled with the redeposition of silica, appears to influence the calculated mass of the quartz sphere at these temperatures. The diameter decreases dramatically causing obvious overestimation of the solubility. A typical trend is exhibited by the data of $\rho = 0.94$ g/ cm^3 (Fig. 4). The experimental curve shoots up vertically between 391° and 395°C. Only one experiment displayed any hint of an equilibrated saturated state (Fig. 6). The triangles in this plot mark a constant solubility, due to very little silica reprecipitation, between 395° and 462°C. The solubility begins to increase again at 490°C at which point considerable reprecipitation, due to a temperature fluctuation within the HDAC, is observed. Therefore, we may attribute the overestimation of our quartz solubility to two different factors: (1) the reprecipitation of a silica phase and (2) the refaceting of the quartz sphere. This information has not been incorporated into the optical weighing program and should be included in the calculations in future experiments. We conclude that this optical weighing method, in its present state, is limited in determining quartz solubility up to ~370°C.

It is clear that in situ analyses offer the experimentalist a very valuable tool in obtaining real observations at experimental conditions. In the case of hydrothermal systems, the advent of the HDAC has certainly opened and improved new opportunities in geochemistry. Zotov and Keppler (2002) were the first to use the HDAC to measure silica solubility. Not only were they successful in reproducing previously published data (Fournier and Potter, 1982; Manning, 1994), they were also able to quantify silica speciation by probing the sample chamber with a laser and collecting micro-Raman spectra of the solution. Our solubility study at lower temperatures and pressures using an optical weighing method, essentially a sample weight-loss method without the need for sample quench, also correlates well with published data by Manning (1994). This novel approach to in situ measurements has its limitations as noted above but nonetheless reveals the potential for continuing investigations in the HDAC; in particular, low temperature solubility and growth experiments, as well as morphologic and possible kinetic studies.

Acknowledgments—The authors would like to thank Dr. Don Davis and Dr. Yuri Amelin for their assistance with quartz abrasion and development of the optical weighing method. We would also like to thank Mr. George Kretschmann for his technical support with the heat controllers, and Dr. W.A. Bassett for his help with the HDAC. GSH and JMB thank the Natural Sciences and Engineering Research Council (NSERC) of Canada for discovery and equipment grants. We also thank three anonymous referees for their comments and constructive criticism of our manuscript.

Associate editor: W. Casey

REFERENCES

Anderson G. M. and Burnham C. W. (1965) The solubility of quartz in supercritical water. *Am. J. Sci.* **263,** 494–511.

Bassett W. A., Shen A. H., Bucknum M., and Chou I.-M. (1993) A new diamond anvil cell for hydrothermal studies to 2.5 GPa and from −190 to 1200C. *Rev. Sci. Instrum.* **64,** 2340–2345.

Brady E. L. (1953) Chemical nature of silica carried by steam. *J. Phys. Chem.* **57,** 706–710.

Fournier R. O. and Potter R. W., II. (1982) An equation correlating the solubility of quartz in water from 25 to 900°C at pressures up to 10,000 bars. *Geochim. Cosmochim. Acta* **46,** 1969–1978.

Frederickson A. F. and Cox J. E. Jr. (1954) Mechanism of "solution" of quartz in pure water at elevated temperatures and pressures. *Am. Mineral.* **39,** 886–900.

Friedman I. I. (1948) The solubility of quartz in sodium carbonate solutions at high temperature. *J. Am. Chem. Soc.* **70,** 2649–2650.

Heimann R., Franke W., and Willgallis A. (1970) The kinetics and morphology of the dissolution of quartz. Part IV: Dissolution in alkaline environments under supercritical conditions. *N. Jb. Miner. Mh.* **2,** 74–83.

Kennedy G. C. (1950) A portion of the system silica-water. *Econ. Geol.* **45,** 629–653.

Kennedy G. C., Wasserburg G. J., Heard H. C., and Newton R. C. (1962) The upper three-phase region in the system SiO_2-H_2O. *Am. J. Sci.* **260,** 501–521.

Kitahara S. (1960a) The solubility of quartz in water at high temperatures and high pressures. *Rev. Phys. Chem. Jpn.* **30,** 109–114.

Kitahara S. (1960b) The solubility equilibrium and the rate of solution of quartz in water at high temperatures and high pressures. *Rev. Phys. Chem. Jpn.* **30,** 122–130.

Laudise R. A. and Ballman A. A. (1961) The solubility of quartz under hydrothermal conditions. *J. Phys. Chem.* **65,** 1396–1400.

Manning C. E. (1994) The solubility of quartz in H_2O in the lower crust and upper mantle. *Geochim. Cosmochim. Acta* **58,** 4831–4839.

Matthews W. and Davis W. J. (1999) A practical image analysis technique for estimating the weight of abraded mineral fractions used in U-Pb age dating. In *Radiogenic Age and Isotopic Studies: Report 12,*pp. 1–7. Current Research 1999-F. Geological Survey of Canada.

Mizutani S. (1970) Silica minerals in the early stage of diagenesis. *Sedimentology* **15,** 419–436.

Morey G. W. and Hesselgesser J. M. (1951a) The solubility of some minerals in superheated steam at high pressures. *Econ. Geol.* **46,** 821–835.

Morey G. W. and Hesselgesser J. M. (1951b) The solubility of quartz and some other substances in superheated steam at high pressures. *Am. Soc. Mech. Eng. Trans.* **73,** 865–875.

Morey G. W., Fournier R. O., and Rowe J. J. (1962) The solubility of quartz in water in the temperature interval from 25 to 300C. *Geochim. Cosmochim. Acta* **26,** 1029–1043.

Rimstidt J. D. (1997) Quartz solubility at low temperatures. *Geochim. Cosmochim. Acta* **61,** 2553–2566.

Rimstidt J. D. and Barnes H. L. (1980) The kinetics of silica-water reactions. *Geochim. Cosmochim. Acta* **44,** 1683–1699.

Saul A. and Wagner W. (1989) A fundamental equation for water covering the range from the melting line to 1273 K at pressures up to 25000 MPa. *J. Phys. Chem. Ref. Data* **18,** 1537–1564.

Semenova A. I. and Tsiklis D. S. (1970) Solublity of silicon dioxide in steam at high pressure and temperatures. *Russ. J. Phys. Chem.* **44,** 1420–1422.

Siever R. (1962) Silica solubility, 0–200°C and the diagenesis of siliceous sediments. *J. Geol.* **70,** 127–150.

Smith F. G. (1958) Transport and deposition of the non-sulphide vein minerals. VI. Quartz. *Can. Mineral.* **6,** 210–221.

Sommerfeld R. A. (1967) Quartz solution reaction: 400–500C, 1000 bars. *J. Geophys. Res.* **72,** 4253–4257.

Van Lier J. A., De Bruyn P. L., and Overbeek J. T. (1960) The solubility of quartz. *J. Phys. Chem.* **64,** 1675–1682.

Von Damm K. L., Bischoff J. L., and Rosenbauer R. J. (1991) Quartz solubility in hydrothermal seawater: An experimental study and equation describing quartz solubility for up to 0.5 M NaCl solution. *Am. J. Sci.* **291,** 977–1077.

Walther J. V. and Orville P. M. (1983) The extraction-quench technique for determination of the thermodynamic properties of solute complexes: Application to quartz solubility in fluid mixtures. *Am. Mineral.* **68,** 731–741.

Weill D. F. and Fyfe W. S. (1964) The solubility of quartz in H_2O in the range 1000–4000 bars and 400–500C. *Geochim. Cosmochim. Acta* **28,** 1243–1255.

Zotov N. and Keppler H. (2002) Silica speciation in aqueous fluids at high pressures and high temperatures. *Chem. Geol.* **184,** 71–82.